ELSEVIER

Cement & Concrete Composites 25 (2003) 867–872

Cement & Concrete Composites

www.elsevier.com/locate/cemconcomp

A thermodynamic model for predicting the stability of thaumasite

I. Juel [a,*], D. Herfort [a], R. Gollop [b], J. Konnerup-Madsen [c], H.J. Jakobsen [d], J. Skibsted [d]

[a] *Aalborg Portland A/S, P.O. Box 165, 9100 Aalborg, Denmark*

[b] *Lafarge Technical Directorate, 305 London Road, Greenhithe, Kent DA9 9JQ, UK*

[c] *Geological Institute, University of Copenhagen, Øster Voldgade 10, 1350 Copenhagen K, Denmark*

[d] *Department of Chemistry, Instrument Centre for Solid-State NMR Spectroscopy, University of Aarhus, Langelandsgade 140, 8000 Århus C, Denmark*

Abstract

A model based on the phase rule has been used to predict the hydrate phase mineralogy and phase proportions from the chemical composition of hydrated Portland cement altered by sulfate attack. The eight-component system on which the model is based consists of CaO, SiO_2, Al_2O_3, Fe_2O_3, MgO, $CaSO_4$, $CaCO_3$ and H_2O. The phases included in the model are C–S–H, portlandite, ettringite, hydroxy-AFm, monosulfate, monocarbonate, calcite, gypsum, thaumasite, brucite and the pore solution. The model predicts, among other things, that thaumasite, which forms at low temperature, is unstable in the presence of AFm phases, and can only form in systems that would otherwise form gypsum at higher temperatures. The model has been tested experimentally on cement pastes containing 15 and 30 wt.% limestone dust stored at 5 °C, and which were either mixed with different amounts of gypsum and stored in water, or stored in solutions of different $MgSO_4$ concentrations. The fully hydrated pastes have been analysed by XRD and ^{29}Si CP/MAS NMR, whilst the remaining solution was analysed by ICP. Thaumasite is only found in regions where it has been predicted to form as a stable phase.

Keywords: Thaumasite; Phase rule; Portland cement; Limestone

1. Introduction

Concrete damage from thaumasite formation has caused growing concern in the UK over recent years [1]. Thaumasite formation has also been reported in numerous other countries across the cooler regions of the northern hemisphere [2–4]. It is generally accepted that the requirements for the thaumasite form of sulfate attack (TSA) in Portland cement systems involve a supply of sulfate and carbonate ions, high humidity and temperatures below 15 °C [5–7].

The British ''Thaumasite Expert Group'' [1] noted that ''The range of quantities of soluble sulfates, required for TSA in not precisely known''. Herfort et al. [8] showed that, although thaumasite does not contain Al_2O_3, cements with higher aluminate contents should offer the greatest resistance to TSA, since more sulfate is required before thaumasite formation is made possible. This goes against conventional wisdom where higher Al_2O_3 contents are normally regarded as posing a greater risk of deleterious ettringite formation.

Earlier investigations on the stability and formation of thaumasite have shown that high amounts of gypsum added to the cement [7], or interactions between cement and sulfate rich solutions [9], can lead to thaumasite formation in limestone blended cements. In a systematic study by Hartshorn et al. [10] small paste specimens consisting of Portland cement blended with different amounts of limestone filler were stored at low temperature in $MgSO_4$ and Na_2SO_4 solutions for several months before testing. Unfortunately, however, since the solution was replaced at regular intervals total chemical composition was not controlled. Although some sub-systems such as the $CaO–Al_2O_3–CaSO_4–H_2O$ and $CaO–Al_2O_3–CaSO_4–CaCO_3–H_2O$ systems have been investigated under equilibrium conditions at constant composition e.g. [11,12], the only multi-component systems relevant to thaumasite formation which have been studied in this way were reported by Herfort et al. [8]. This study investigated the hydrate phase assemblages of limestone Portland cements at high sulfate contents which were increased, either through addition

* Corresponding author. Tel.: +45-98777051; fax: +45-98164741.
E-mail address: iaj@aalborg-portland.dk (I. Juel).

0958-9465/$ - see front matter © 2003 Elsevier Ltd. All rights reserved.
doi:10.1016/S0958-9465(03)00114-8

of gypsum, or storage in $MgSO_4$ solutions. Unfortunately, insufficient gypsum was added for it to persist as a stable phase at 20 °C, which as argued in [8] is a prerequisite for the formation of thaumasite at low temperature. Thaumasite was, therefore, only found in specimens stored at 5 °C in $MgSO_4$ solutions for which the total composition was sufficiently over-sulfated for gypsum to occur at normal temperature. The goal of the investigation described here is to repeat the investigations described in [8] over a wider range of composition including over-sulfated systems obtained by addition of both gypsum and $MgSO_4$.

2. Model description

The model is based on the phase rule which states that $P + F = C + 2$, where P is the number of phases, F is the number of degrees of freedom, and C is the number of components chosen to describe the system. By assuming equilibrium conditions in a hydrated Portland cement paste, the phase assemblage, including the relative contents of phases, can be accurately predicted from the chemical composition of the hydrated system and some knowledge of the stability of the relevant hydrate phases at relevant temperatures and pressure. These calculations essentially involve solving n equations for n unknowns, where the unknowns are the relative contents of phases in wt.%, and where each equation corresponds to one of the chemical components, i.e. CaO for the first equation, Al_2O_3 for the second equation, etc. For example in the $CaO–Al_2O_3–CaSO_4–H_2O$ quarternary system, the first equation may be given as $CaO_{Ett} \cdot Ett + CaO_{MS} \cdot MS + CaO_{CH} \cdot CH + CaO_{PS}.PS = CaO_{SYS} \cdot 100$, where Ett, MS, CH and PS are the contents of ettringite, monosulfate, portlandite and pore solution in wt.%, CaO_{Ett}, CaO_{MS}, CaO_{CH} and CaO_{PS} are the weight fractions of CaO in each of these phases, and CaO_{SYS} is the weight fraction of CaO in the system, or sample being studied. Three additional equations can be constructed for each of the additional three components giving four equations and four unknowns which is used to calculate the relative contents of phases present. The same approach can be extended to eight equations and eight unknowns for the eight-component system investigated in this study.

The chemical components chosen were CaO, SiO_2, Al_2O_3, Fe_2O_3, MgO, $CaSO_4$, $CaCO_3$, although the model can be extended even further to include alkalis and other minor components. The hydrate phases included in the model were C–S–H, portlandite, ettringite, monosulfate, monocarbonate, FH_3 ($Fe_2O_3 \cdot 3H_2O$), calcite, gypsum, thaumasite and brucite. The model can be modified to include other phases such as hydrogarnet and hydrotalcite which may be more stable than the AFm phases and brucite in the long term. In the calculations it is assumed that the hydrate phases have standard stoichiometric compositions, except for C–S–H which in the presence of portlandite was fixed at $1.7CaO \cdot SiO_2 \cdot 0.05Al_2O_3 \cdot 4H_2O$. This composition is based on the results from Young and Hansen in [13] and electron microprobe analyses (not included here) which showed the C–S–H phase to contain minor Al_2O_3 corresponding to the amount indicated.

The calculations described above can be performed incrementally at increasing sulfate contents, and used to predict the phase stabilities and mineralogical zoning resulting from sulfate attack. The result of this type of approach is shown in Fig. 1 for a blend initially consisting of Portland cement and 15 wt.% raw feed precipitator dust. The raw feed precipitator dust consists primarily of calcite. Thaumasite is assumed to be a stable phase in the example given corresponding to reaction at low temperature. At temperatures higher than 15 °C thaumasite is unlikely to form [1]. Gypsum forms instead when all the available Al_2O_3 has reacted with sulfate to form ettringite. The initial composition of the cement and the dust is given in Table 1. The Figure

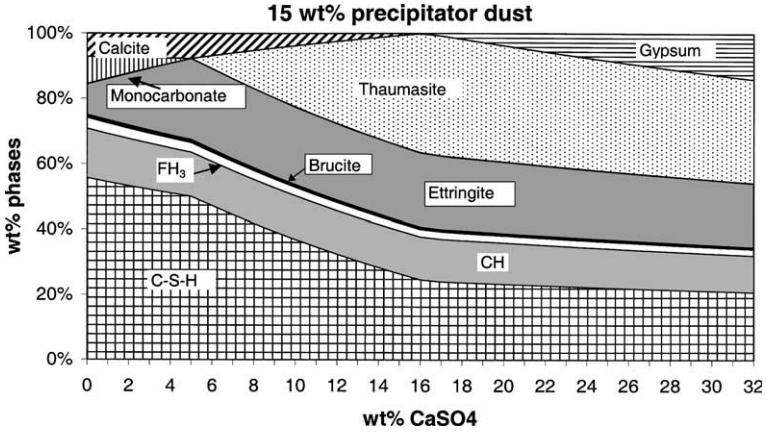

Fig. 1. The phase composition of a blended cement with 15 wt.% raw feed precipitator dust shown as a function of the $CaSO_4$ content. Thaumasite is assumed to be a stable phase. Abbreviations: FH_3, $Fe_2O_3 \cdot 3H_2O$.

Table 1
Composition and physical data for the cement and limestone filler used (all values are in wt.% except for the SSA values which are in m^2/g)

	SiO_2	Al_2O_3	Fe_2O_3	CaO	SO_3	MgO	CO_2	SSA	0.045 mm	LOI
Cement	21.17	5.07	3.87	64.13	2.93	0.89	0	374	2.86	0.8
Filler	10.93	3.01	1.67	46.64	0.26	0.55	35.56	1227	<1	35.56

shows that an addition of about 5 wt.% $CaSO_4$ is required for initial thaumasite formation to occur. The addition of about 17 wt.% $CaSO_4$ is necessary to form gypsum in the presence of thaumasite.

The incompatibilities of thaumasite and monocarbonate, gypsum and calcite etc. implicit in the example shown in Fig. 1 are more easily visualised in the ternary sub-system shown in Fig. 2. The components chosen ($CaSO_4$, $CaCO_3$ and C_3A) are valid as long as they occur as stoichiometric units in all phases. C_3A includes the total Al_2O_3 content of the system. FH_3. Although some iron may be incorporated in the AFm and AFt phases, the model assumes FH_3 to be the sole reaction product containing iron. Evidence in the literature that at least some of the iron forms FH_3 is compelling ([13, p. 185–186]). Applying the phase rule to the ternary subsystem, which only allows three phases (for an invariant assemblage at constant temperature and pressure), thaumasite can clearly only form at sulfate contents necessary to form gypsum at higher temperatures, i.e. above the ettringite–calcite tie-line. Unlike the situation at high temperature, calcite and gypsum cannot coexist in the presence of thaumasite. Fig. 2 also shows why Al_2O_3 rich systems containing fly ash or slag tend to be most resistant to thaumasite related damage since higher contents of sulfate would be required to form thaumasite. The figure also shows why sulfate resisting Portland cement should be least resistant.

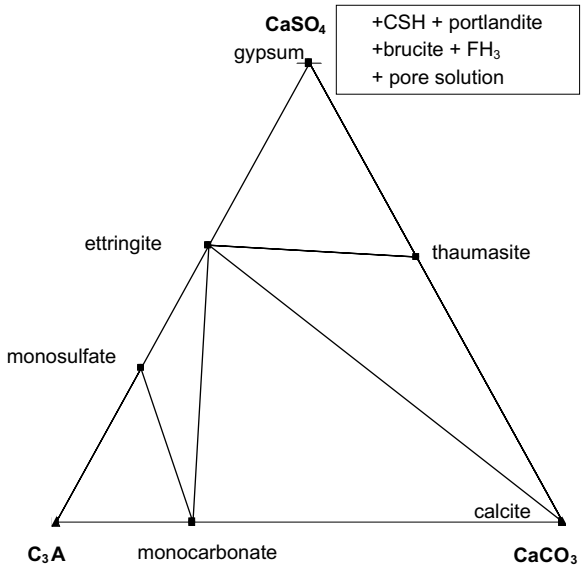

Fig. 2. Projection of the relevant phases on to sub-ternary compatibility diagram for the C_3A–$CaCO_3$–$CaSO_4$ system showing the relative contents of the phases.

The absence in the literature (to the best of our knowledge), of reports on assemblages including both monocarbonate and thaumasite supports the view that these two phases are incompatible. Based on this model, unstable assemblages, such as those containing thaumasite + gypsum + ettringite + calcite reported by Gaze and Crammond [14], must represent non-equilibrium conditions.

3. Experimental

3.1. Specimen preparation

The model described above was tested experimentally on cement pastes prepared from an ASTM type II cement replaced by 15 and 30 wt.% raw feed precipitator dust. The compositions and fineness of the cement and dust are shown in Table 1. Pure analytical gypsum and $MgSO_4 \cdot 7H_2O$ were used to adjust the sulfate content.

Four series of pastes were prepared. The composition of the samples in the first two series (Series 1 and 2) included 15 and 30 wt.% dust by weight of the anhydrous cement + dust. After 5–10 days of hydration the specimens were immersed in $MgSO_4$ solutions of increasing concentration The remaining two series (Series 3 and 4) also included 15 and 30 wt.% dust, but with additions of gypsum ranging up to 30.5 wt.% $CaSO_4$ by weight of the cement + dust. An overview of the samples is given in Table 2.

The cement and dust (and gypsum in series 3 and 4) were blended before mixing with water.

The paste specimens were mixed at a water/binder ratio of 0.7 and cast in small plastic cylinders 8 mm in diameter and 35 mm in length, giving a volume of approximately 2 cm^3. For the first three days the specimens were stored at 40 °C and rotated continuously to avoid bleeding. After demoulding the specimens were transferred to 18 cm^3 plastic cells with room enough for three specimens in each cell. The cells were then filled with approximately 12 ml solution, either freshly boiled distilled water or $MgSO_4$ solution, and stored at 5 °C. The concentrations of the $MgSO_4$ solutions used in the series 1 and 2 pastes were calculated to give the total compositions shown in Fig. 3a and in Table 2. Likewise, the contents of gypsum added to the series 3 and 4 blends were calculated to give the compositions shown in Fig. 3b and Table 2. The solution surrounding the paste

Table 2
Contents of $MgSO_4$, $CaSO_4$ and limestone dust in wt.% of the anhydrous cement + dust

Filler	Series/sample	A	B	C	D	E	F	G	H	I
15	1 ($MgSO_4$)	1.8	7.1	12.4	15.9	21.2	–	–	–	–
30	2 ($MgSO_4$)	0	3	6	12	18	21	24	27	30
15	3 ($CaSO_4$)	2	8	14	18	24	–	–	–	–
30	4 ($CaSO_4$)	0	3.4	6.8	13.6	20.4	23.7	27.1	30.5	–

specimens is essentially identical to the pore solution, and its composition is solely dependent on the equilibrium hydrate phase assemblage in question (making allowances for the dilution of alkalis). The samples were stored for at least five months prior to analysis.

The water in the specimen cells was filtered from the samples under vacuum, using 45 micron glass filter paper. The pH was determined by a pH electrode, at either 10 or 100× dilution depending on the amount of solution available for analysis. Two drops of concentrated HNO_3 were added to the solutions, which was then stored at 5 °C till further analysis. Sub-samples for X-ray diffraction (XRD) and scanning electron microscopy (SEM)/electron probe microanalysis (EPMA) analysis were placed in a vacuum chamber at 40 °C. The samples for XRD analysis were removed after approximately 1 h. The samples for ^{29}Si cross-polarization magic angle spinning nuclear magnetic resonance (CP/MAS NMR) were kept at 5 °C prior to analysis.

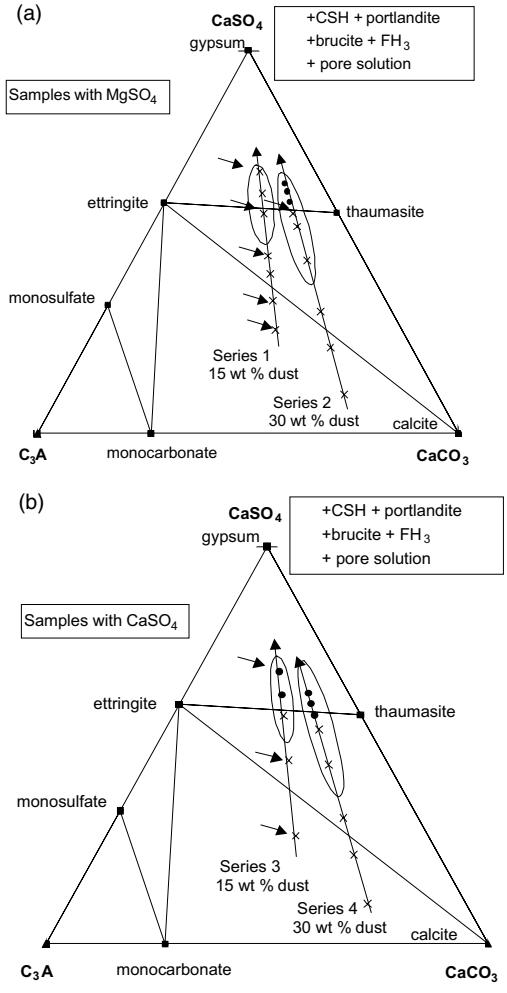

Fig. 3. (a) Samples with $MgSO_4$ and (b) samples with $CaSO_4$. The composition of paste specimens plotted in the $CaSO_4$–C_3A–$CaCO_3$ sub-system. The samples analysed by NMR are indicated by arrows. Samples where thaumasite is identified are encircled. Samples where gypsum is identified are indicated by filled circles. In Table 2 the samples within each series are given the letters A, B, C... with increasing amounts of $MgSO_4/CaSO_4$.

3.2. ^{29}Si CP/MAS NMR

The ^{29}Si CP/MAS NMR spectra were recorded at room temperature on a Varian INOVA-400 spectrometer using a home-built CP/MAS NMR (nuclear magnetic resonance) probe for 7 mm o.d. rotors. The ^{29}Si CP/MAS NMR spectra employed a spinning speed of $\nu_r = 3.0$ kHz, a 800 μs CP contact time, a 8 s relaxation delay, and typically 4096 scans. The quantities of thaumasite were determined from these spectra using the method described in detail by Skibsted et al. [15].

3.3. XRD

The specimens were crushed to 53 μm in a glove box with a nitrogen atmosphere and analysed using a Siemens D5005 X-ray diffractometer. Acceleration voltage: 40 kV, current: 40 mA, stepsize: 0.01° 2θ, time/step: 1 s, slit: variable slit v12, Cu Kα radiation.

3.4. Solutions

The concentration of SO_4^{2-}, Ca^{2+}, K^+ and Na^+ was determined using a Perkin Elmer Optima 3000 ICP, with a solid state charged coupled detector and a radial orientated torch. The calibration curves for all elements always had a correlation coefficient better than 0.999 and typically a value around 0.9999 or better. Both XRD and ICP analyses were performed at Blue Circle's Technical Centre, Greenhithe, UK.

4. Results and discussion

The phase assemblages identified by XRD and ^{29}Si CP/MAS NMR are shown in Table 3 together with data

Table 3
Ternary phase assemblages identified by the XRD and ^{29}Si CP/MAS NMR in addition to pore solution data from ICP analysis

Sample	Phase assemblage within the ternary sub-system		Solution composition, mmol/l				
	Predicted	Identified	SO_4^{2-}	Ca^{2+}	K^+	Na^+	pH
1a	Cc Mc Ett	Cc Mc Ett	0.16	5.8	17.3	15.3	12.5
1b	Cc Th Ett	Cc Ett	0.46	13.1	18.4	16.1	12.4
1c	Cc Th Ett	Cc Th Ett	1.4	5.1	18.1	16.1	12.4
1d	G Th Ett	Cc Th Ett	1.8	5.1	19.0	17.0	12.5
1e	G Th Ett	Cc Th Ett	3.3	2.0	22.2	19.8	12.6
2a	Cc Mc Ett	Cc Mc Ett	0.16	5.9	15.4	13.3	12.5
2b	Cc Mc Ett	Cc Mc Ett	0.30	21.9	16.6	14.3	12.3
2c	Cc Th Ett	Cc Mc Ett	0.23	7.5	11.6	10.0	12.3
2d	Cc Th Ett	Cc Th Ett	1.1	5.4	15.3	13.4	12.6
2e	Cc Th Ett	Cc Th Ett	2.0	4.7	17.7	15.5	12.3
2f	Cc Th Ett	Cc Th Ett	2.1	4.1	18.3	16.0	12.1
2g	G Th Ett	Cc Th Ett	7.1	5.0	22.1	20.1	12.1
2h	G Th Ett	Cc G Th Ett	11.9	10.2	23.4	21.9	12.3
2i	G Th Ett	Cc G Th Ett	13.5	10.1	22.1	19.8	12.1
3a	Cc Mc Ett	Cc Mc Ett	0.16	5.8	18.0	15.8	12.5
3b	Cc Th Ett	Cc Ett	0.14	5.4	17.7	16.0	12.4
3c	Cc Th Ett	Cc Th Ett	3.2	6.6	15.6	14.0	12.3
3d	G Th Ett	Cc G Th Ett	8.4	9.3	15.9	14.9	12.3
3e	G Th Ett	Cc G Th Ett	8.8	10.1	15.0	13.8	12.2
4b	Cc Mc Ett	Cc Mc Ett	0.16	5.1	16.5	14.5	12.3
4c	Cc Th Ett	Cc Ett	0.24	6.0	16.0	14.4	12.1
4d	Cc Th Ett	Cc Th Ett	3.5	7.3	14.4	13.2	12.2
4e	Cc Th Ett	Cc Th Ett	8.7	11.4	14.1	13.4	12.0
4f	Cc Th Ett	Cc G Th Ett	8.8	11.7	13.5	12.8	11.9
4g	G Th Ett	Cc G Th Ett	8.9	12.2	12.8	12.1	12.0
4h	G Th Ett	Cc G Th Ett	9.5	11.9	14.3	14.0	12.2

Portlandite was identified in all specimens by XRD, whilst brucite was found in most series 1 and 2 specimens. C_4AF contents identified in most samples were generally too low to significantly affect the results. Abbreviations: Cc, calcite; Mc, monocarbonate; Ett, ettringite; Th, thaumasite; G, gypsum.

Table 4
Quantities of thaumasite in wt.% calculated from the model and determined by ^{29}Si CP/MAS NMR

Sample	1A	1B	1C	1E	2F	3A	3B	3E
Calculated	0	7	21	26	50	0	7	25
Measured	0	0	2.7	16.3	11.7	0	0	9.5

for the solutions. The quantities of thaumasite found by ^{29}Si CP/MAS NMR are shown in Table 4. The phase assemblages identified are in general agreement with those predicted by the model shown in Fig. 3a and b with the following notable exceptions.

Calcite occurs in all samples even in the presence of gypsum and thaumasite. Since this violates the phase rule, it cannot represent an equilibrium assemblage. The most likely explanation is the inability of over-sized calcite grains to completely react in the time available.

Thaumasite begins to form at higher contents of sulfate than predicted by ternary phase diagrams shown in Fig. 3a and b. This may, at least in part, be explained by some incorporation of sulfur in the C–S–H phase, and/or the incorporation of some iron in ettringite. This is currently being investigated by the present authors using EPMA analysis. Initial formation of gypsum also takes place at higher than expected sulfate contents in the samples stored in $MgSO_4$. The significance of these results is that they confirm the model in terms of the minimum sulfate content required for thaumasite formation as defined by the tie-line joining ettringite and calcite in Fig. 3a and b. For a normal Portland cement this tie-line corresponds to between 7% and 10% SO_3 by weight of the anhydrous cement, depending on the carbonate and aluminate contents. Thaumasite will, of course, form at lower sulfate contents in systems containing less aluminate, e.g. in systems containing sulfate resisting cement, whilst higher sulfate contents would be required to form thaumasite in aluminate rich systems, e.g. those produced from slag or fly ash cements. Apart from the hypothetical case of an over-sulfated sulfate

resisting cement, thaumasite cannot form from the sulfates already present in the cement, regardless of the content of carbonates, and some external source of sulfate would invariably be required. The fact that thaumasite formed at higher sulfate contents than the threshold values corresponding to the ettringite–calcite tie-line in Fig. 3a and b, can be explained by the incorporation of some iron in the AFt and or AFm phases rather than as FH_3. This remains to be investigated.

The compositions of the solutions (which are essentially identical to pore solution albeit with low alkali contents) are shown in Table 3. Compositions for the solutions in equilibrium with the assemblages which, either do not include thaumasite, or contain gypsum, are in good agreement with data found in the literature (e.g. [13]), making allowances for the different alkali contents and temperature. SO_4^{2-} concentrations in the solutions at equilibrium with calcite + ettringite + monocarbonate (+excess phases) range, for most samples, between 0.1 and 0.2 mmol/l. SO_4^{2-} concentrations in the solutions at equilibrium with ettringite + thaumasite + gypsum (+excess phases) range, on the whole, from 8 to 12 mmol/l, whilst SO_4^{2-} concentrations in the solutions coexisting with thaumasite without gypsum range from 1 to 3 mmol/l. The latter is in good agreement with the pore solution compositions found in the presence of thaumasite by Herfort et al. in [8]. The characteristic sulfate concentration in solutions at equilibrium with thaumasite may be a valuable diagnostic parameter in identifying the presence of thaumasite, particularly at low contents in the absence of gypsum.

5. Conclusions

The experimental results presented are consistent with the model which predicts that thaumasite can only form in Portland cement based systems at sulfate contents high enough to form gypsum at normal temperature. This invariably requires an external source of sulfates regardless of the carbonate content.

Slag and fly ash cements should offer greatest resistance to thaumasite related attack owing to their high aluminate contents, whilst sulfate resisting cements are expected to offer least resistance.

Limits on the Al_2O_3 or C_3A contents in sulfate resisting cement intended to minimise the risk of external sulfate attack may be counter-productive in the presence of carbonates and sufficiently low temperatures to stabilise thaumasite.

Acknowledgements

The authors would like to thank Peter Hugget, John Pettit and Garreth Pugh for their invaluable assistance to I. Juel during his stay with them at the Blue Circle Technical Centre in Greenhithe.

References

[1] Report of the Thaumasite Expert Group. The thaumasite form of sulfate attack: risks, diagnosis, remedial works and guidance on new construction. Department of the Environment, Transport and the Regions, England, 1999.
[2] Bensted J. Mechanism of thaumasite sulphate attack in cements, mortars and concretes. Zement-Kalk-Gips 2000;12(53):704–9.
[3] Rogers C, Thomas M, Lohse H. Thaumasite from Manitoba and Ontario, Canada. In: Proceedings of the 19th International Conference on Cement Microscopy, 1997. p. 306–19.
[4] Hagelia P, Sibbick RG, Crammond NJ, Grønhaug A, Larsen CK. Thaumasite and subsequent secondary calcite deposition in sprayed concretes in contact with sulfate bearing Alum shale, Oslo, Norway. In: Proceedings of the 8th Euroseminar on Microscopy Applied to Building Materials, 2001. p. 121–30.
[5] Bensted J. Scientific background to thaumasite formation in concrete. World Cem 1998;(11):102–5.
[6] Crammond NJ. Thaumasite in failed cement mortars and renders from exposed brickwork. Cem Concr Res 1985;(15):1039–50.
[7] Gaze ME. The effects of varying gypsum content on thaumasite formation in a cement:lime:sand mortar at 5 °C. Cem Concr Res 1997;(27):259–65.
[8] Herfort D, Porsborg AT, Grundvig S, Jakobsen HJ, Skibsted J. Hydrate phase assemblages of Portland cement pastes stored at 5 and 20 °C. In: Proceedings of the 20th IOM Cement and Concrete Science Conference, 2000.
[9] Borsoi S, Collepardi S, Coppola L, Collepardi M. Sulfate attack on blended Portland cements. In: Proceedings, Fifth CANMET/ACI International Conference on Durability of Concrete, supplementary paper 192-26, 2000. p. 417–32.
[10] Hartshorn SA, Sharp JH, Swamy RN. Thaumasite formation in Portland–limestone cement pastes. Cem Concr Res 1999;(29):1331–40.
[11] Kuzel H-J, Pöllmann H. Hydration of C_3A in the presence of $Ca(OH)_2$, $CaSO_4 \cdot 2H_2O$ and $CaCO_3$. Cem Concr Res 1991;(21):885–95.
[12] Damidot D, Glasser FP. Thermodynamic investigation of the $CaO–Al_2O_3–CaSO_4–H_2O$ system at 25 °C and the influence of Na_2O. Cem Concr Res 1993;(23):221–38.
[13] Taylor HFW. Cement chemistry. 2nd ed. London: Thomas Telford; 1997.
[14] Gaze ME, Crammond NJ. The formation of thaumasite in a cement:limestone:sand mortar exposed to cold magnesium and potassium sulphate solutions. Cem Concr Comp 2000;(22):209–22.
[15] Skibsted J, Hjorth L, Jakobsen HJ. Quantification of thaumasite in cementitious materials by $^{29}Si\{^1H\}$ cross-polarization magic-angle spinning NMR spectroscopy. Adv Cem Res 1995;26(7):69–83.